



Publication Year	2015
Acceptance in OA	2020-04-24T11:02:12Z
Title	Thermal control system of the Exoplanet Characterisation Observatory Payload: design and predictions
Authors	MORGANTE, GIANLUCA, TERENCE, LUCA, Eccleston, P., Bradshaw, T., Crook, M., Linder, M., Hunt, T., Winter, B., FOCARDI, MAURO, MALAGUTI, GIUSEPPE, MICELA, Giuseppina, Pace, E., Tinetti, G.
Publisher's version (DOI)	10.1007/s10686-015-9469-7
Handle	http://hdl.handle.net/20.500.12386/24223
Journal	EXPERIMENTAL ASTRONOMY
Volume	40

Thermal control system of the Exoplanet Characterisation Observatory Payload: design and predictions

G. Morgante¹ · L. Terenzi^{1,10} · P. Eccleston² · T. Bradshaw³ ·
M. Crook³ · M. Linder⁴ · T. Hunt⁵ · B. Winter⁵ · M. Focardi⁶ ·
G. Malaguti¹ · G. Micela⁷ · E. Pace⁸ · G. Tinetti⁹

Received: 24 June 2014 / Accepted: 25 June 2015
© Springer Science+Business Media Dordrecht 2015

Abstract The Exoplanet Characterisation Observatory (EChO) is a space mission dedicated to investigate exoplanetary atmospheres by undertaking spectroscopy of transiting planets in a wide spectral region from the visible to the mid-InfraRed (IR). The high sensitivity and the long exposures required by the mission need an extremely stable thermo-mechanical platform. The instrument is passively cooled down to approximately 40 K, together with the telescope assembly, by a V-Groove based design that exploits the L2 orbit favourable thermal conditions. The visible and short-IR wavelength detectors are maintained at the operating temperature of 40 K by a dedicated radiator coupled to the cold space. The mid-IR channels, require a lower

✉ G. Morgante
morgante@iasfbo.inaf.it

¹ INAF - IASF Bologna, via P. Gobetti,101, 40129 Bologna, Italy

² RAL Space, STFC Rutherford Appleton Laboratory, Harwell Campus, Didcot OX11 0QX, UK

³ Technology Department, STFC Rutherford Appleton Laboratory, Harwell Campus, Didcot OX11 0QX, UK

⁴ Science and Robotic Exploration Directorate, European Space Agency, ESTEC, Keplerlaan 1, 2200 Noordwijk, The Netherlands

⁵ Mullard Space Science Laboratory, Holmbury St. Mary, Dorking, Surrey RH5 6NT, UK

⁶ INAF - Osservatorio Astrofisico di Arcetri, Largo E. Fermi 5, I-51025 Firenze, Italy

⁷ INAF - Osservatorio Astronomico di Palermo, Piazza del Parlamento 1, 90134 Palermo, Italy

⁸ Dip. di Fisica ed Astronomia, Università di Firenze, Via Sansone, 1, 50019 Sesto Fiorentino (FI), Florence, Italy

⁹ Department of Physics and Astronomy, University College London, London WC1E 6BT, UK

¹⁰ Facoltà di Ingegneria, Università degli Studi e-Campus, via Isimbardi 10, 22060 Novedrate (CO), Italy

operating temperature and are cooled by an active refrigerator: a 28 K Neon Joule-Thomson (JT) cold end, fed by a mechanical compressor. Temperature stability is one of the challenging issues of the whole architecture: periodical perturbations must be controlled before they reach the sensitive units of the instrument. An efficient thermal control system is required: the design is based on a combination of passive and active solutions. In this paper we describe the thermal architecture of the payload with the main cryo-chain stages and their temperature control systems. The requirements that drive the design and the trade-offs needed to enable the EChO exciting science in a technically feasible payload design are discussed. Thermal modelling results and preliminary performance predictions in terms of steady state and transient conditions are also reported. This paper is presented on behalf of the EChO Consortium.

Keywords Exoplanets · EChO · Space instrumentation · Thermal control · Cryogenics · Infrared

1 Introduction

One of the main topics of the ESA Cosmic Vision 2015–2025 programme was related to the question: *what are the conditions for planet formation and the emergence of life?* Exoplanet discoveries in the recent years have profoundly changed our understanding of the formation, structure, and composition of planets. Current surveys from space and ground telescopes show that the majority of stars have planets that range in size from sub-Earths to larger than Jupiter. The incredible variety of the characteristics (orbits, dimensions, temperature, composition, atmosphere, etc.) these objects show indicates that planetary systems appear much more diverse than expected.

A space project has been studied to take up the challenge to explain this diversity. The Exoplanet Characterisation Observatory (EChO) [1] is the first mission dedicated to investigate exoplanetary atmospheres with the objective of providing answers to the Cosmic Vision question, addressing the suitability of those planets for life and placing our Solar System in context. Proposed as a candidate for the Medium Class M3 opportunity of the ESA Cosmic Vision programme in 2014, EChO is designed to undertake spectroscopy of transiting exoplanets over the widest wavelength range possible, providing high resolution, multi-wavelength spectroscopic observations on the atmospheres of a large and representative selected sample of known exoplanets. These observations will allow the compositions, temperature, albedo, size and variability to be determined at a level never previously attempted. This information will allow to constrain models of their internal structure and improve our understanding of how planets form and evolve.

1.1 Mission and payload description

EChO is designed as a survey mission for transit and eclipse spectroscopy capable of observing a large planet sample within its four-year mission lifetime [2]. The spacecraft (S/C) will be launched on board the Soyuz launcher from the *Centre Spatial Guyanais* in Kourou (French Guyana), into a direct transfer leading to a large amplitude orbit around the Sun-Earth L2 (second Lagrangian point). This science operations orbit is

key to meeting two of the most important requirements: it offers a very stable environment (for thermal, power and communication purposes), combined with a very large instantaneous field of regard. The launch window shall be constrained according to two major thermal requirements:

- no eclipses during the mission lifetime for thermal and power generation stability
- minimal sun exposition of the PLM during launch to avoid over-heating of sensitive instrumentation

The spacecraft has a wet mass of about 1.6 t and a solar array power generation capability of about 1 kW.

In Fig. 1 is reported a possible pictorial view of the EChO spacecraft together with a block diagram showing the basic mission concept: a cold Payload Module (PLM) mounted on a warm Service Module (SVM) [3]. The SVM contains all the units required to support the payload and instrument in operating conditions (the Warm Electronics system [4]) and to keep all S/C services operational. The PLM, supported on the SVM by three fiberglass reinforced plastic (GFRP) bi-pods, includes the thermal shielding system: three V-Grooves [5] that, in sequence, are used to passively cool the telescope assembly and the instrument to <45 K to minimize the thermal background and the noise of the focal plane detectors. The telescope assembly is composed by an optical bench, the baffle and the telescope: a three mirror elliptical off-axis Korsch design [3] providing an effective collecting area of 1.131 m² and a small collimated input beam to the instrument. The observation sequence consists of staring mode spectroscopic observations taken over the various phases of the target light curve [2]: the spectrum of the planet is seen either in absorption against the stellar spectrum (primary transit) or in emission together with that of the star. The stellar spectrum is observed in the absence of the planet as the planet transits behind the star (secondary eclipse). For this reason, there is no need for a large field of view, nor for high angular resolution and a 1 m² class telescope is sufficiently large to achieve the necessary spectrophotometric precision.

The signal from the planet is isolated from the star by fitting a light curve to each observation as the planet transits in front and behind the host star. Extracting the spectrum of the planet therefore requires the co-addition of many transit observations

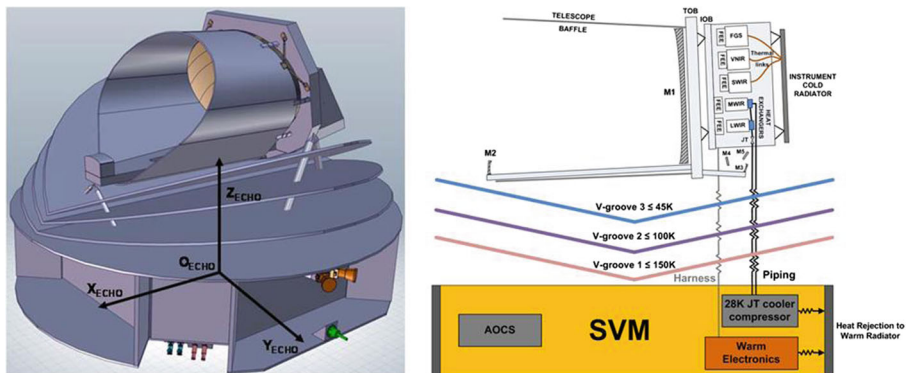


Fig. 1 Pictorial view (*left*) and block diagram (*right*) of the EChO spacecraft

in order to build up the total signal to noise ratio in the measurement. To reach the level of sensitivity required demands a high level of stability in the detection system, that, in turn, can be achieved only with a very careful payload design. This is particularly true with regard to factors that can affect the photometric stability of the system and/or generate spurious signals. In this framework, thermal design is one of the key issues of systematic errors control.

The payload is completed by the Instrument Focal Plane Unit (Fig. 2): the Instrument Optical Bench (IOB) with the instrument module channels, the instrument radiator and the cryogenic system cold ends for detectors cooling, and the fine guidance sensor (FGS) needed to achieve the fine pointing stability required [3]. A shroud encloses the whole instrument unit shielding from straylight contamination and radiative thermal contributions.

1.2 Instrument

The scientific objectives of the mission require a broad instantaneous wavelength coverage to detect as many molecular species as possible, to probe the thermal structure of the planetary atmospheres and to correct for the contaminating effects of the stellar photosphere. The baseline instrument is a single integrated, but modular, three channel, high stability spectrometer that covers the full EChO required wavelength range of 0.55 to 11.0 μm in a compact optical arrangement. The instrument configuration includes (Figs. 2 and 3 left) a cross-dispersed spectrometer VNIR (Visible and Near IR) module with two fibre-fed channels covering from 0.55 to $\sim 2.5 \mu\text{m}$ (with the goal of extending

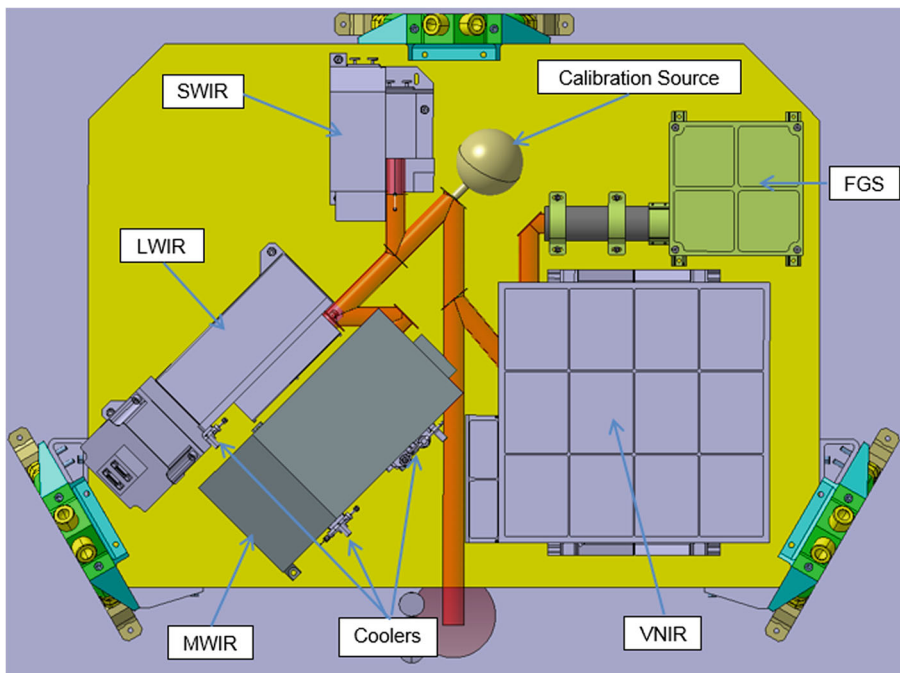


Fig. 2 EChO PLM mechanical configuration on the Instrument Optical Bench

the range down to $0.4 \mu\text{m}$), a grism spectrometer SWIR (Short Wavelength IR) module covering from 2.5 to $5.3 \mu\text{m}$, and a prism spectrometer module with two MWIR (Mid Wavelength IR) channels, imaged on a single focal plane, covering the 5.05 – $11.5 \mu\text{m}$ range (5.05 – $8.65 \mu\text{m}$ and 8.25 – $11.5 \mu\text{m}$). A fourth extra Long Wavelength IR (LWIR) channel covering the 11 – $16 \mu\text{m}$ range is part of the general design as a goal. The channel boundaries were chosen to ensure overlapping of spectral ranges between modules for full wavelength coverage and cross-calibration (Fig. 3 right). The spectral resolving power needed, $R \sim 300$ for wavelengths less than $5 \mu\text{m}$ and $R \sim 30$ for wavelengths greater than this, is achieved or exceeded throughout the band. The spectrometer channels share a common field of view, with the spectral division operated by a dichroic chain.

The baseline selection of detectors for all channels is MCT (Mercury Cadmium Telluride) coupled to SIDECAR ASIC-type Front End Electronics (FEE) [3, 4]. The FGS, VNIR and SWIR channels are based on Teledyne H2RG devices, operating at a temperature of about $\sim 40 \text{ K}$. This is achieved passively with a dedicated instrument cold radiator. The M/LWIR detectors reach the required dark current and detector noise level at a temperature of $\sim 28 \text{ K}$, that is provided by an active refrigerator based on a Neon Joule-Thomson cooler [3].

2 Thermal architecture

The spacecraft thermal design (Fig. 4) is based on a cold Payload Module (PLM) sitting on the top of a warm Service Module (SVM). The mission thermal control is ensured by a combination of passive and active cooling systems. The SVM is thermally controlled in the 260 K – 280 K range for nominal operations of all the S/C subsystem units. This is achieved through panel radiators on the module sides that constantly face the cold sky and dedicated heaters where required. Thermal uniformity across the warm radiators is achieved by heat pipes.

The cold payload is passively cooled by a high efficiency thermal shielding system. The SVM top floor, covered with low emissivity Kapton MLI, acts as the first main barrier between the PLM and the Sun and all warm units in the service module. A set of 3 V-Groove (VG) thermal shields, similar to the configuration in the Planck ESA satellite [5], provides the first three cold reference stages exploiting the favourable conditions of the L2 thermal environment. The VG1, VG2 and VG3 stages operate at temperatures around 150 K , 90 K and 50 K respectively and are used for intercepting parasitic heat leaks (harness, struts, piping, radiation, pre-amplifiers) and for cryo-cooler pre-cooling. The Telescope Assembly, operating in the cold environment

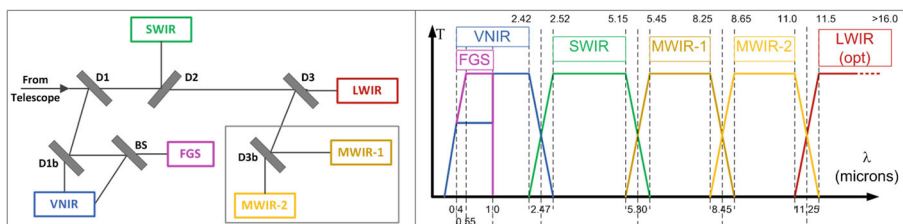


Fig. 3 Echo Instrument channels configuration (*left*) and wavelength ranges splitting (*right*)

Table 1 Main thermal requirements for the EChO Instrument and expected dissipation from cold active units

Channel	Optical modules		Detectors			T control stage		FEE		
	Op T (K)	ΔT^a (K)	Op T (K)	ΔT^a (K)	Load ^b (mW)	Load ^b (mW)	Op T (K)	ΔT^a (K)	Load ^b (mW)	
FGS	≤ 50	0.5	≤ 45	± 0.05	10	5	≤ 55	2	20	
VNIR	≤ 50	0.5	≤ 45	± 0.05	10	5	≤ 55	2	20	
SWIR	≤ 50	0.5	≤ 45	± 0.05	8	5	≤ 55	2	20	
MWIR	≤ 32	0.5	≤ 28	± 0.005	5	5	≤ 55	2	20	
LWIR	≤ 28	0.5	≤ 28	± 0.005	5	5	≤ 55	2	20	

^a Peak to peak value over a typical observation cycle time (10 h)

^b 50 % margin is assumed at this stage of the study

selection, derived from the basic scientific requirements [2], and can be summarized in the following table:

The detectors and front-end electronics load reported in table is evaluated on the basis of the design trade-off study of the channels detecting chain. The control stages power is a maximum average allocation for the predicted dissipation of the closed loop circuit when assumptions on the expected instabilities at the relevant thermal interfaces are made (see section 5).

2.2 PLM thermal design baseline

From a simplified thermo-mechanical point of view, each channel module can be considered as composed by a box, made of an Al alloy to minimize thermal gradients, that includes the optics and a Detector System (DS). Each DS includes the Focal Plane Assembly (FPA) and the Temperature Control Stage (TCS). Due to FPA electrical performance requirements the cryo-harness connecting the FEE to their detectors cannot be longer than 10–20 cm. This means that the cold electronics must be mounted in proximity of the detectors. For the three warmer channels the front end electronics is installed on the module box nearby the detectors stage. For the L/MWIR modules, in order not to over load the cooler cold end, the FEE box is mounted on the Instrument Optical Bench (IOB). The FEE thermal coupling to the modules boxes, or to the IOB, is optimized to allow an efficient heat transfer to the Telescope Optical Bench via the IOB itself.

The general scheme of the EChO thermal architecture, with the six main thermal interfaces, is shown in Fig. 5. The FGS, VNIR and SWIR modules basically share the same thermal design. The detectors operate at $T \leq 45$ K, cooled by a dedicated passive radiator stage (the instrument radiator see section 3.1) located inside the cold environment set by the third V-groove and the Telescope Assembly. This radiator is mechanically supported on the IOB by means of insulating struts and is considered a part of the instrument. High conductive links connect the FGS, VNIR and SWIR detectors, through their thermal control stage, to the radiator. The module boxes of these channels are mechanically and thermally anchored on the instrument bench by using conductive mechanical supports. In this configuration, at steady state, the FGS/VNIR/SWIR

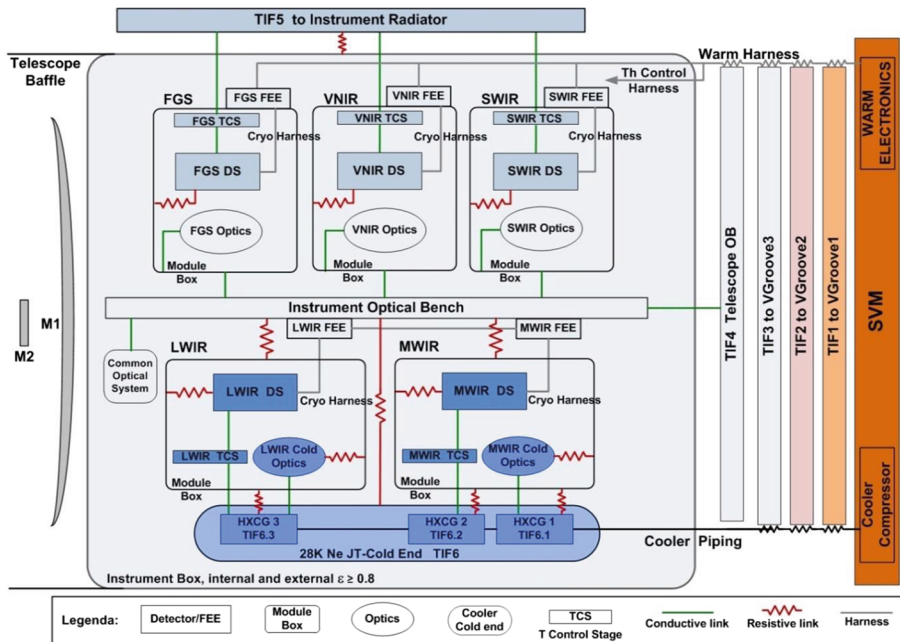


Fig. 5 PLM thermal architecture scheme with main thermal interfaces to S/C

optical units are expected to thermally equilibrate with the IOB. The MWIR and LWIR detectors technology requires a lower operating temperature, on the order of 30 K, to achieve the required sensitivity and noise level. This temperature, when a load of tens of mW is dissipated, can be reached only by using an active cryocooler. The baseline for the refrigeration system is described in section 3.2. The MWIR and LWIR module optics shall operate at low temperature, to minimize thermal background noise on the detectors. For this reason the modules boxes and part of the internal optical units needs to be thermally decoupled from the optical bench, to limit the heat load on the cooler heat exchangers. The optimization of the longer wavelength channels cooling requires that the MWIR and LWIR modules and the cooler cold ends are located in a compact mechanical arrangement to minimize the thermal path (see Figs. 2 and 5). For this reason, the JT cooler cold tip is split in three heat exchangers (HXCG 1, 2 and 3) mounted at a convenient position on the modules by insulating supports. Detectors and cold optics connect to these cold references by high conductivity thermal links. Since the LWIR channel cold optics and detectors share the same temperature requirements a single heat exchanger serves the whole module. Two separate heat exchangers are dedicated to the MWIR optics and detectors, since they should work at different temperatures.

In general, each detector stage is thermally decoupled from the relative module box or optics, to ensure optimal performance in terms of absolute temperature and stability. Coupling of the detectors to the temperature reference stage (cooler cold end or radiator) is achieved through high conductance links (high purity Al straps) that interface the focal plane Thermal Control Stage (TCS). This is composed by the detector supporting flange that integrates the active closed loop thermal control system:

a heater plus thermistor couple driven by the Instrument Control Unit (ICU) [4] of the warm electronics.

Instrument radiative thermal control is achieved by shielding with the proper IR emissivity. The radiative environment for the modules is set by the instrument enclosure, defined by the IOB and the box: a shroud that surrounds the channel modules and the common optics to shield them from the external environment. The radiative coupling between subsystems inside the box is defined by the high IR emissivity requirement ($\epsilon \geq 0.8$) needed to minimize straylight radiation contamination in the optical paths of the channels. The mechanical units (boxes and surfaces) inside the cavity are externally coated with black paint or anodizing. For the same reason the box needs low emissivity on the external surface and high emissivity internally. This is achieved by using low ϵ Multi-Layer Insulation (MLI) on the outside and black coated MLI inside. The instrument cavity is passively maintained at a temperature ≤ 45 K by the radiative background set by the V-Grooves and the Telescope Assembly.

The warm electronics is located in the SVM. All harness from SVM to instrument channels should be thermally linked to all the passive stages (VG1, VG2, VG3 and TOB) for maximum parasitic interception. In this way the heat leaks due to wiring on the cooling stages are minimized. For the warmer channels (VNIR and SWIR) the harness can be used as a conductive link: if the cables are thermally anchored to the colder TOB they can efficiently transfer heat from the cold electronics towards the telescope assembly. The harness heat leaks to detectors is controlled by a proper thermal design of the cabling (see section 2.4).

2.3 Thermal interfaces and hardware

For a cryogenic instrument, internal and external thermal interfaces optimization is the key to a successful design. In the EChO instrument configuration six main Thermal Interfaces (TIF's) to the S/C and PLM have been identified (see Fig. 5) together with many others internal to the units. Instrument performance is ensured by flowing the basic instrument requirements (Table 1) down to the main thermal interfaces. The resulting requirements must ensure best performance of the optical and detector systems over longer periods and full mission lifetime.

The required conductance values at the EChO TIF's have been evaluated and bounded by running parametric analysis in the thermal model simulations. A typical value of $500 \text{ W/m}^2\text{-K}$ is assumed as the average surface thermal conductance of machined metallic interfaces when they comply to the specifications typical of flight hardware. This value, for example, was achieved in several Planck couplings in the 20–45 K range even with M4 bolts, using spring washers and, in some cases, a filler (gold sheet). In general, the required conductance values at interfaces can be achieved using common materials and solutions already adopted in previous experiments (e.g. Planck and JWST-MIRI [5, 6]): GFRP or carbon-fibre reinforced plastic (CFRP) for insulating struts and 5 N purity Al for the high conductivity links. Standard Al alloys (such as 6061) are used for most of the instrument structures and boxes. Stainless steel bolts (A2-70) not smaller than M5 are assumed for the main mechanical couplings to spacecraft and to the optical bench. In general, to optimize the thermal contact, the maximum bolt dimension allowed by the mechanical allocations and design is used. If

needed, spring washers and a thermal filler (gold or indium sheets) can be considered to improve conductance.

FGS, VNIR and SWIR module boxes are coupled to the optical bench by conductive Al struts: with $500 \text{ W/m}^2\text{-K}$, 10 cm^2 of total contact surface allow a conductance of 0.5 W/K , more than enough to ensure a good thermal coupling given the small heat fluxes across those interfaces. The MWIR/LWIR modules are insulated from the IOB by sized stainless steel (304 L or 316 L) stands that reach resistance values on the order of 10^3 K/W . The detectors are thermally decoupled from their modules and the IOB by insulating supports to improve their stability, while thermal contact with the cooling stage (cold end or cold radiator) is optimized. The FPA insulation from the module box is ensured by small bipods in CFRP, such as T300, that allow a thermal conductance on the order of 10^{-4} W/K while ensuring mechanical stiffness.

The thermal coupling of the detectors with their temperature reference (cooler or radiator) is achieved via their active control system that operates as an intermediate stage between FPA and cooling point. The TCS coupling to both sides must be carefully optimized to find the best trade-off between maximum conductance and minimum control power as these two conditions go in opposite directions. The control stage should be partially decoupled to act as a passive filter by increasing the system time constant and to minimize the power needed for active control. The better the coupling to the cooling stage, the higher the power for thermal control. The optimal conductance for the EChO control stages has been evaluated by thermal model analysis. A conductance on the order of 0.1 W/K between the thermal control system and their cooling stage is the best compromise, while an order of magnitude lower is needed for the coupling to the detector ($G \sim 0.01 \text{ W/K}$). Each FPA (Fig. 6) is supported on the control flange by 316 L (G1 in the figure) stainless steel stands sized to achieve the required total 0.1 W/K . The 0.01 W/K (G2) links needed to connect the detector control stages to their operating temperature reference are based on high purity Al straps. The total conductance G2 between the radiator or cold end and the detectors, results from the combination in series of the strap, flanges and contact resistance at the interfaces. The design of these thermal links was optimized taking into account the correction factors for the typical inefficiencies in the density of foils per unit area, in the effective length of the link (due to complex routing) and in the welds of the foils to the end flanges. Exploiting the high thermal conductivity of pure Al at low temperatures, it is possible to limit the section of each straps to $\sim 50 \text{ mm}^2$ for

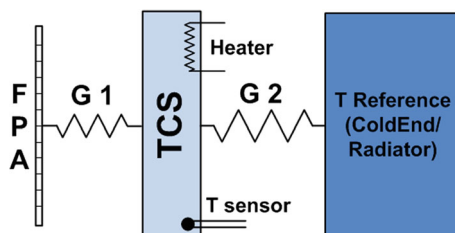


Fig. 6 Detector modules thermal control stage scheme

a total mass of all links on the order of 1 kg. Short straps connect the M/LWIR to the cooler cold end heat exchangers while the FGS, VNIR and SWIR need longer links (in the 70–100 cm range) to reach the interface points on the cold radiator and require a more complex routing of the straps.

The EChO scientific performances require high stability and a careful control of possible systematic error sources during observations, in particular thermal emission and temperature oscillations. The active thermal control hardware consists of thermistors and heaters. Detailed temperature monitoring is achieved by the combination of direct measurements with units thermal prediction analysis, correlated with all ground test results at sub-system and system level. A thermistor is installed in correspondence of each critical interface or node. The total number of thermometers adds up to 30 units (plus full redundancy). Temperature measurements are based on Cernox sensors scanned at 1 Hz: a resolution of at least 25 mK and an accuracy of 50 mK are required in the units operational range. The thermistors used for detectors thermal control should have a resolution of at least 10 mK for the VNIR and SWIR and 1 mK for the M/LWIR detectors in a narrow (few K) range around the operating temperature. All thermistor are read in twisted pairs 4-wires measurement configuration by the readout electronics [4]. Heaters are needed for thermal control of the channels detector. A total of 5 nominal (plus 5 redundant) heaters are integrated on the detector thermal control stages, one per channel. The heaters are controlled by the ICU with feed-back closed loop logic. Heaters power supply is on the spacecraft 28 V line and they are capable of providing up to 2 W for decontamination and in case detectors annealing process is needed. The thermal control range is 0–20 mW with a resolution of 100 μ W. All heaters are connected to the control electronics by shielded twisted pairs to minimize EMI.

2.4 Harness thermal analysis

In the EChO instrument, detectors wiring and service harness (general housekeeping, thermal control heaters, thermistors etc.) consist of a high number of electrical connections. In cryogenic instruments harness design is a critical issue, not only for the electrical performance but also for the thermal balance of the whole system. A reliable harness electrical design needs to optimize the speed of acquisition and detectors driving signals while minimizing losses. This defines the cable design in terms of wire size, electrical properties, shielding configuration etc. At the same time, for thermal reasons, a functional cabling baseline should be capable of ensuring the lowest heat leaks. Best electrical performance is achieved by using highly conductive materials that, on the other side, are very good thermal conductors. The EChO harness is designed to comply as much as possible to both conflicting requirements.

Minimization of harness parasitic heat leaks from the warm units to colder stages is typically pursued in two ways:

- appropriate selection of materials combined with an optimal combination of gauge wiring and harness length
- maximum heat leak interception on intermediate passive stages (V-Grooves, TOB, IOB)

In the EChO PLM two main groups of harness can be identified:

- the detector modules harness composed by
 - the wires that connect the Warm Electronics (WE) to the Cold Front End Electronics (CFEE)
 - the cabling that links the CFEE to the detectors
- the control harness
 - thermal control harness
 - calibration sources control harness

From the thermal point of view, five main sections of the EChO harness can be identified, corresponding to the thermal breaks between the main stages: a simplified scheme of the EChO harness from the SVM to the PLM units is shown in Fig. 7.

The thermal stages temperatures correspond to:

- SVM at 280 K
- V-Groove 1 at 150 K
- V-Groove 2 at 100 K
- V-Groove 3, IOB and TOB for simplicity are considered to be all at the same temperature of 50 K (worst case assumption, as the TOB and IOB can be colder than the last V-Groove)

The thermal break length of the harness section between stages is assumed to be 0.5 m with perfect thermal contact on both sides.

A wide set of possible harness configurations with different materials and wire gauges have been analysed. Among these, few options have been identified and an ad hoc baseline finally selected. The objective of this baseline is to show that a harness thermal design minimizing heat leaks while ensuring optimal detectors control is

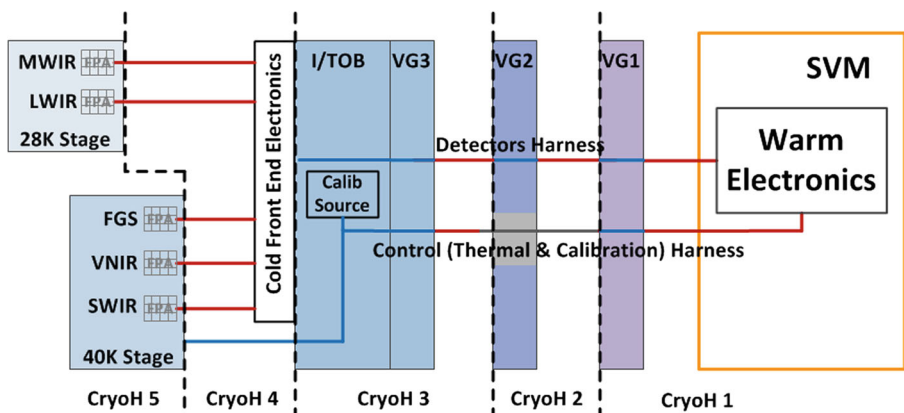


Fig. 7 EChO cryo-harness thermal scheme. Blue lines indicate the isothermal sections, red line show the thermal breaks

possible and technically feasible. The radiative loads exchanged with the environment have been neglected as the harness can be shielded. PTFE or polyester materials, used as electrical insulators in the harness design, can be ignored in the thermal analysis as their contribution to the heat leak is negligible.

The selected material and wire gauge combination that best suits the EChO set of requirements from both the electrical and thermal point of view are:

- CuZn (brass) AWG 30 for bias control and power supply (to detectors and thermal control heaters)
- PCuSn (Phosphorous Bronze) AWG 36 and stainless steel (SS) AWG 36 for analog and digital I/O and all other signals (thermistors and calibration sources control)
- braids of AWG 44 stainless steel wires are used for cable shielding

The final configuration for the harness from the warm electronics to the cold front ends is based on a single cable per channel with the following assumptions:

- LVDS standard (TBC) 37 pins micro-D connector, 1 round bundle cable per channel
- Shielding baseline:

all twisted pairs configuration

stainless steel cable over shielding (braids made by a matrix of AWG44 wires)

stainless steel internal shielding (matrix of AWG44 wires), one for each quadruplet (two pairs)

For each configuration it is checked that the electrical resistance over the cables results low enough to ensure the electrical performance. The trade-off between thermal and electrical requirements shall be taken at a higher level of detail in a next phase of design, as the number of connections, the requirements on resistivity and losses, the size of the wires, the currents, voltages and frequencies used, the shielding needs, all depend on the data acquisition strategy, on frame clock rate and on the detectors control techniques. For these reasons, a 91 pins/wires harness configuration, based on nano-D connectors, is studied as a possible backup to the above summarized baseline. In this case, the extra load in terms of heat leak would not be dramatic as by decreasing the wire gauge it is possible to double the number of wires with a net increase in conducted load of less than 30 %.

The harness connecting the Sidecars to the detectors is typically based on flexi circuit harness. Due to the short length required for system performance (in the 0.1 to 0.2 m range) this link is a critical issue for the thermal balance of the instrument. A possible baseline configuration that might ensure electrical performance while meeting heat loads allocation on the coldest stages has been studied. The main assumptions are:

- one flat flexi cable per channel with 37 pin micro-D connector
- harness length 0.2 m
- stainless steel cable over shielding (braids based on a matrix of AWG44 wires)

The instrument control harness connects thermal control units (thermistors and heaters) and the calibration source to the Instrument Control Unit in the SVM. Thermistor readout is based on 4-wires measurement: for this reason electrical resistance along the lines is less important and more thermally insulating materials can be used. Heaters control and power supply, on the other side, will require lower resistivity to minimize power losses and Joule heating effects. The instrument control harness represents the major contribution because of the high number of connections.

Thermistors:

- 30 Instrument and cryo-cooler thermistors, fully redundant (total is 60) in the cold PLM
- 4 wires readout, a total of 240 wires
- stainless steel AWG 36 wires in twisted pairs

No shielding, except for the twisted pair configuration, is assumed for the thermistors cabling. In case, it would be possible to shield thermistor cables every twisted quadruplet with SS AWG44 jackets. This increases the heat leak to the 150 K, 100 K and 50 K stages by 25 % and to the 40 and 28 K stages by 3 %.

Heaters:

- 10 heaters (nominal+redundant) for thermal control
- 2 brass AWG 30 wires each, for a total of 20 wires
- twisted pairs plus stainless steel shielding over each pair

Calibration units:

- 2 bundle cables (one for the common IR source, one for the VNIR source) of 4 brass AWG 30 and 12 P-CuSn AWG36 wires each, for a total of 16 wires each cable
- twisted pairs plus stainless steel shielding over each pair

The total loads of the EChO harness on the main thermal stages can be summarized in Table 2.

The expected harness heat leaks on PLM passive stages seem to be within spacecraft allocations. The resulting heat load on the coldest stages (Cold Radiator and JT cold end) is well inside the allocated 10 mW. The margins can be used to sustain possible ohmic and radiative extra loads, or extra shielding if needed. A reduction of the

Table 2 Total harness load on stages

Load on stages	VG1 150 K (mW)	VG2 110 K (mW)	VG3 50 K (mW)	Instrument radiator 40 K (mW)	Cooler coldend 28 K (mW)
Harness total load	194.77	58.27	41.03	3.45	4.43
Total load w/30 % margin	253.21	75.75	53.34	4.49	5.76

conducted load could be achieved by using smaller gauge wires (AWG32/AWG38) or other materials (Manganine for example) for the 4-wires measurement connections (thermistors). In this way it could be possible to decrease thermal harness parasitic loads by a factor of ~ 2 .

These numbers should be seen as a reference case, to be used as guidelines for a possible evolution of the instrument design. There is still some margin to reduce the loads by a proper trade-off design activity, minimizing wires number, size and material. Cable shielding also shall be carefully evaluated as it may easily become the dominating effect from a thermal point of view. A more realistic thermal optimization of the cryo-harness will be possible only once the instrument design will be more advanced in all other aspects.

3 Instrument cooling stages

3.1 40 K passive stage: the instrument radiator

The V-Groove shields design provides a cold environment (~ 50 K) for the PLM units: telescope, instrument and cryocooler. The VNIR, SWIR and FGS detectors require a colder (below 45 K) and more stable reference. This is achieved by a dedicated radiator for detectors cooling only. This extra passive stage, referred as Instrument Radiator, is developed under the responsibility of the Instrument Consortium. The design process starts from the main assumptions (Table 1) in terms of temperature and load for the channel detectors linked to the radiator. The V-Grooves heat rejection capacity is used to intercept parasitic heat leaks to the cold stage: harness, struts and radiation from warmer units. In this way this cold radiator is fully devoted to channel detectors cooling, with parasitic loads generated only by its own supporting struts and thermal control harness. The expected total detector dissipation from all three channels is around 43 mW. The radiator is mounted on the Instrument Optical Bench (IOB); if the total conductance of the radiator struts to the IOB is on the order of 0.005 W/K (using 304 L stainless steel bipods) the expected conductive load on the radiator is around 60 mW even in the hot case temperature boundary (55 K). This value can be dramatically reduced by using more insulating materials for the bipods such as GFRP or CFRP. Harness heat leak allocation is 10 mW. In total, 115 mW (including margin) is the expected load to the cold radiator, in the worst case.

The PLM configuration allows to fit a radiator of nearly 1 m^2 on the back of the Instrument Box. After several iteration in the EChO thermo-mechanical design process, a radiant surface of 0.96 m^2 (shape and dimensions are shown in Fig. 8) has been modelled, fully enclosed in the radiative environment defined by the last V-Groove and the Telescope Optical Bench. The orientation angle of the radiator inside the allocated volume is around 20° with respect to the vertical direction.

The radiator thermo-mechanical design is based on a sandwich of Al6061 (TBC) alloy layers (Fig. 9). A honeycomb cell structure 3 cm thick, with 2 cm cell size and ribbon thickness of 1 mm, is packed between two 2 mm thick layers. This simple thermo-mechanical design allows for low mass and volume while ensuring at the same time mechanical rigidity and good thermal conductance in all three directions. The

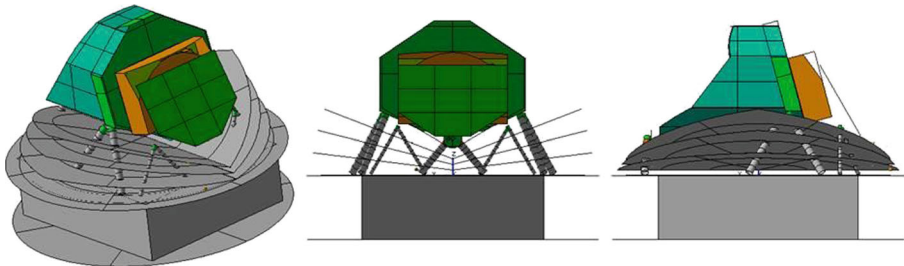


Fig. 8 Configuration of the instrument radiator on PLM

system is mechanically supported on the IOB with three bipods made of 304 L stainless steel thin wall tubes.

The radiator can be coated with white paint to avoid overheating due to a possible exposure to the Sun during launch. For this reason a conservative IR emissivity of 0.8 is assumed for this study even if white coatings with emissivity over 0.9 are available and regularly adopted for space applications. The radiator emissivity and efficiency could be furthermore increased by using other standard solutions on the external surface (special coatings, honeycomb structure etc.). On the radiator internal surface facing the PLM, a low emissivity shroud limits radiation loads from the warmer parts of the spacecraft.

A 35 nodes simple thermal model dedicated to radiator performance has been developed. The three channel detectors with their active loads that include T control dissipation and thermal harness heat leaks are connected to the central node to study the worst case in terms of temperature distribution and gradients. An extra harness leak due to radiator thermal control harness is also simulated on an adjacent central node. Finally the parasitic loads due to struts are also simulated by evaluating the contribution of three bipods made of 304 L stainless steel. The radiator is then coupled to cold deep space on the basis of the above reported assumptions. On the internal side, an emissivity of 0.05 is assumed. The boundaries (IOB and PLM cavity) are set at the worst, hot case, value of 55 K.

In Fig. 10 the simulated temperature distribution is reported. The radiator max temperature gradient is around 200 mK, showing a very good uniformity even in this

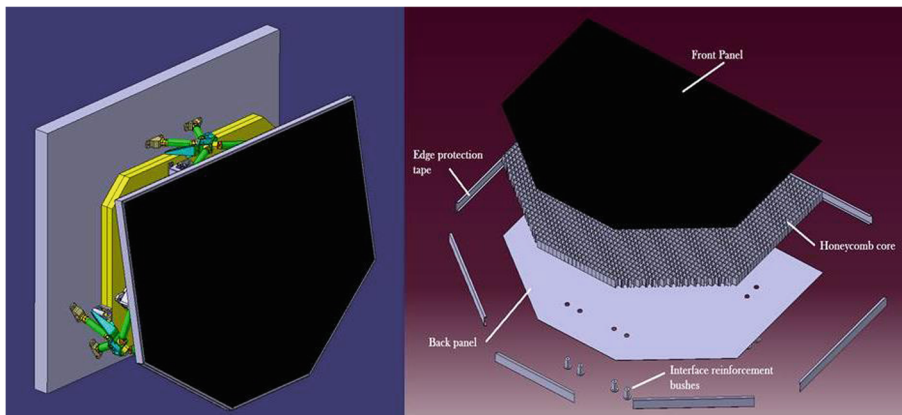


Fig. 9 CAD view of: Cold Radiator on the IOB (*left*), sandwich structure (*right*)

conservative configuration. In order to improve spatial gradient results, a more symmetrical distribution of the loads dissipated on the radiator can be arranged.

3.2 28 K active stage: JT cooler

The EChO JT cryo-cooler has been designed by the RAL Cryogenics and Magnetics group in the UK. The baseline for the active cooling system is a Joule-Thomson cooler making use of the cold heat exchangers (HXCG) developed for the Planck mission [5] and the advanced compressor systems designed by RAL as part of a 2 K cooler system developed by the RAL team under a contract with ESA. With a required operating temperature of 28 K for the coldest stage it was decided to use Neon as the working cryogen. Its boiling point of 27.05 K at 1 atmosphere and its melting point of 24.55 K allow only a very narrow operating range when working with Ne and this restricts the possible reference temperature interval. For the EChO system [3] the JT shall be constantly operated at slightly above 1 bar on the low pressure side.

A schematic view of the cooling system configuration is shown in Fig. 11. The system incorporates a compressor stage that boosts the gas pressure from around 1.1 bar to 11 bar. One of the main features of the 2 K compressor modular system is that the design can be easily adjusted (in terms of piston diameter, stroke, input power etc.) to suit different operating requirements. Initial modelling shows that the EChO requirements could be met by a two stage system, essentially using only half of the 2 K cooler compressor stages shown in Fig. 12 (left panel). The compressed gas at first passes through an ancillary panel where the flow is measured and the gas is cleaned through a getter. The connecting pipework conveys the fluid through the heat exchanger for precooling and filters for trapping impurities on each of the passive stages. Enthalpy is recovered by means of a recuperative tube-in-tube piping that forces the

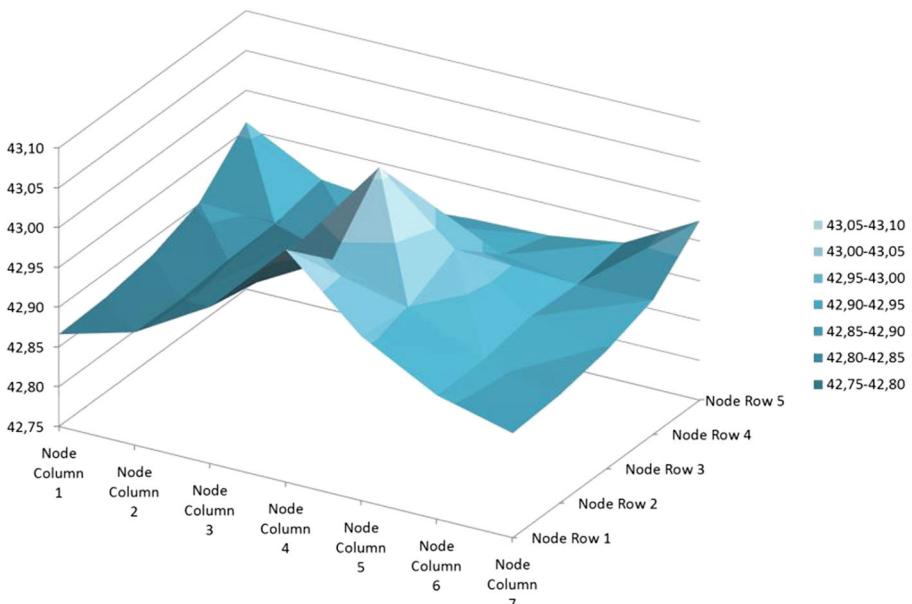


Fig. 10 Radiator 3D temperature distribution

warm high pressure and the cold low pressure streams to exchange heat. Finally the incoming gas enters the JT heat exchanger and one last filter before passing through the expansion orifice where liquid is formed (Fig. 12, right). This liquid is contained in a sintered element to prevent sloshing and flash evaporation effects disturbing the temperature stability. On EChO there are several cooling point and these will be served by multiple heat exchangers. The cold gas then returns back to the compressors through the heat exchangers precooling the incoming gas.

The cooler design has been currently sized to provide 200 mW of cooling power at 27 K (Table 3). To achieve this performance approximately 35 mg/s of Ne flow is required at the planned operating pressure drop. This leads to a pre-cooling requirement of approximately 650 mW at the 100 K V-Groove and ~550 mW on the 45 K V-Groove. The input power required to provide this cooling is 130 W including electronics (30 W) and margin.

The compressors (Fig. 11, left) are balanced in that they run in a head to head configuration. Vibration control is a key feature for a mission that requires such high level of stability during scientific observations. The exported vibration from balanced compressors on similar systems has been reduced to around 100 mN with crude amplitude balancing. On the Planck mission, with active vibration control, levels of a few mN were achieved. If required, algorithms that can be used to reduce the 100 mN to lower levels are available and proven.

As the EChO mission lifetime requirement is 4 years with the goal of a possible extension, gas cleanliness is vital to long term operation of a JT cooler. Following the Planck mission positive experience, a careful purge and fill protocol to ensure the gas cleanliness, is key for mission success. In addition, internal materials (outgassing) and components (filters on each cold stage) of the system are selected to ensure a contaminants free fluid loop.

The Cooler Control Electronics (CCE), connected to the +28 V S/C bus via latching current limiters, drives the cryo-cooler compressors, monitors performance and limit

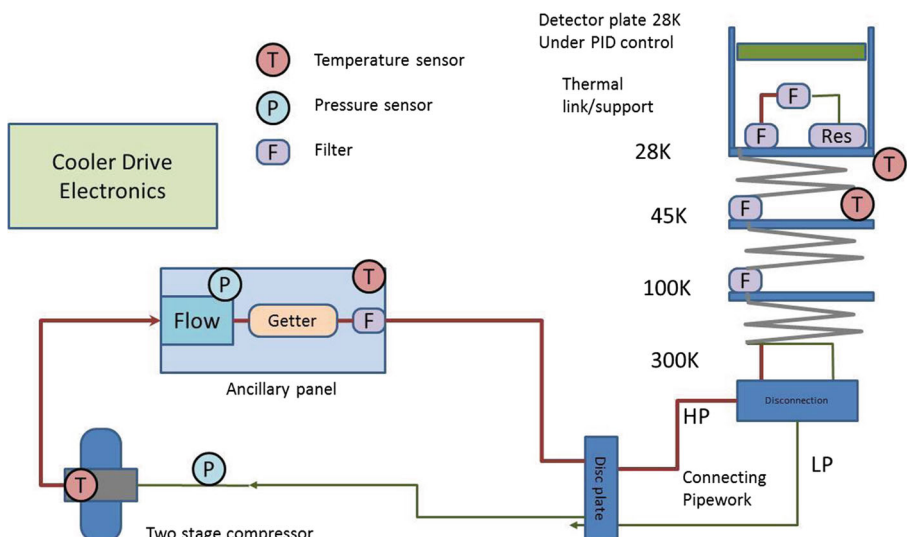


Fig. 11 EChO Active Cooling System configuration

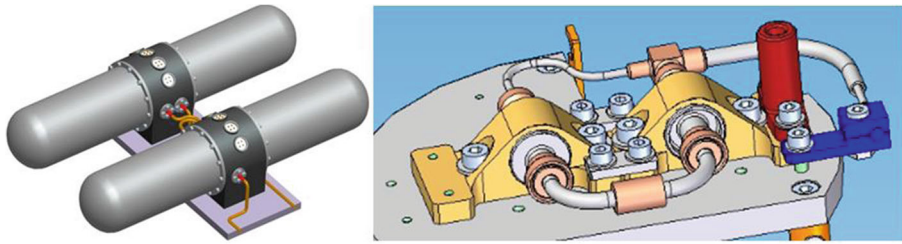


Fig. 12 *Right panel:* drawing of the EChO four stage compressor designed for the 2 K system (EChO system uses half of this). *Left panel:* cryo-cooler filter, expansion valve and liquid reservoir assembly

thresholds, controls the residual exported microvibrations and provides protection as well as housekeeping data. The CCE unit should be located on the SVM as close as possible to the cooler mechanical compressors to limit the length of the high current drive harness which will be delivering of order 100 W to the cooler motors.

4 EChO thermal model

EChO thermal architecture development is based on a set of Thermal Mathematical Models (TMM) [7] used to verify and tune the design solutions. EChO thermal simulations have been carried out in two main steps. First a reduced TMM was used to identify the best thermal configuration of each unit, simulating the instrument behaviour with the PLM interfaces fixed as boundaries. Then the instrument model has been integrated into a geometrical and conductive model of the whole PLM. In this way it was possible to verify the instrument design in the general S/C thermal architecture, simulating realistic interactions and feed-back with the rest of the PLM. Finally the two models have been correlated and adjusted to optimize the design. All simulation have been developed in the ESATAN-TMS environment.

4.1 Reduced TMM

The reduced TMM is used to study the instrument thermal behaviour within the PLM in steady state and its compliancy to the main requirements in terms of temperature, stability and heat fluxes allocated at the internal and external interfaces. The model is composed by a relatively low number of nodes and conductors: the scheme is shown in Fig. 13.

Table 3 Thermal Analysis Heat loads (negative figure indicates cooling)

T stage (K)	Bottom HXCG (mW)	Middle HXCG (mW)	JT HXCG (mW)	JT effect (mW)	Conducted leaks (mW)	Total (mW)
293	-1018.9				-6.7	-1025.6
100	1078.1	-436.1			6.7	648.7
45		593.1	-48.7		0.8	545.1
28				-203.5	0.1	-203.4

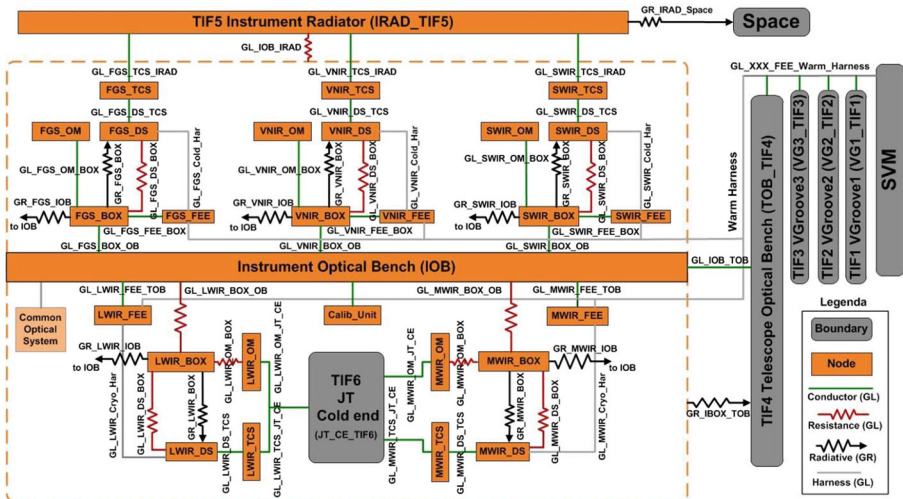


Fig. 13 EChO reduced TMM scheme

The model is based on the best up-to-date assumptions for detectors and electronics dissipations. Each channel module is composed by 5 nodes: the box, the optical system, the detectors, the thermal control stage and the proximity electronics. The instrument cold radiator is a single node coupled to space with properties that replicate the performances of the more detailed model used to simulate the radiator behaviour (see section 3.1). In this reduced steady state model the harness has been simulated as conductive links between stages and units on the basis of the harness thermal analysis (section 2.4). The reduced TMM reproduces the thermal architecture scheme shown in Fig. 5, including the Calibration Unit on the Instrument Optical Bench. The main thermal interfaces are all defined as boundary nodes, with the exception of the IOB that, because of its conductive and radiative coupling with the PLM units, is simulated as a diffusion node.

The model has been run in the expected Hot and Cold thermal cases to bound the range of conductive and radiative environmental conditions. The fixed boundary temperatures for each case are reported in Table 4 together with the model results in terms of nodes temperature and heat fluxes.

The results in terms of temperature distribution are very encouraging: they show very small gradients between the units and the respective interfaces. This yields some extra margin for further optimization of the interfaces. The net heat load across the main thermal interfaces is reported in Table 5.

4.2 PLM conductive and geometrical model

The PLM conductive and geometrical model (Fig. 14) is based on the coupling of a standard M-size SVM configuration with the EChO cold payload. The main radiative surfaces and representative supporting structures between the different stages are simulated on the basis of assumptions derived from the experience of previous successful missions (Planck, Herschel). The final thermal case simulation for the full PLM has been run by integrating the reduced model of the instrument and its radiator in the

Table 4 EChO reduced model nodes results (in bold on grey background the fixed boundaries)

Node name	Q input (W)	T (K)		Node name	Q input (W)	T (K)	
		Cold case	Hot case			Cold case	Hot case
SVM	–	253.0	323.0	SWIR_OM	–	36.8	52.4
VG1_TIF1	–	140.0	150.0	SWIR_DS	0.008	36.1	44.8
VG2_TIF2	–	90.0	110.0	SWIR_TCS	0.005	35.2	42.7
VG3_TIF3	–	35.0	55.0	SWIR_FEE	0.016	37.0	52.5
TOB_TIF4	–	35.0	55.0	VNIR_BOX	–	36.8	52.4
JT_TIF6	–	28.0	28.0	VNIR_OM	–	36.8	52.4
LWIR_BOX	–	34.4	48.9	VNIR_DS	0.01	36.3	45.0
LWIR_OM	–	28.1	28.2	VNIR_TCS	0.005	35.2	42.7
LWIR_DS	0.005	29.8	32.1	VNIR_FEE	0.064	37.0	52.5
LWIR_TCS	0.005	28.2	28.4	FGS_BOX	–	36.8	52.4
LWIR_FEE	0.008	36.9	52.3	FGS_OM	–	36.8	52.4
MWIR_BOX	–	35.1	50.2	FGS_DS	0.01	36.3	45.0
MWIR_OM	–	28.1	28.2	FGS_TCS	0.005	35.2	42.7
MWIR_DS	0.005	29.8	32.1	FGS_FEE	0.064	37.0	52.5
MWIR_TCS	0.005	28.2	28.4	IOB_BOX	–	36.8	52.4
MWIR_FEE	0.008	36.9	52.3	Calib_Unit	0.0018	36.8	52.4
SWIR_BOX	–	36.8	52.4	IRAD_TIF5	–	34.9	42.1

geometrical one. The instrument and radiator nodes definition in terms of bulk materials and properties is based on the reduced model assumptions but with a greater level of detail to deal with the full model interfaces definition. The cold-end at 28 K is represented as a single boundary inside the instrument box. The instrument optical units and detectors are completely enclosed by the instrument bench and box that, at steady state, are basically isothermal. For this reason, the radiative exchange loads with the surroundings are negligible with respect to the conductive fluxes to/from the interfaces. Conductors representing the designed thermal passive links have been added between the instrument units and their respective temperature reference (the IOB, the cold Radiator, the JT cold end). The current version of the model is composed by nearly 1000 nodes. A more detailed description of the full model and its results is available in the EChO mission proposal technical document pack [7].

Table 5 Reduced TMM heat fluxes at the Instrument main thermal interfaces. The uncertainty on these numbers evaluated at this stage of the design process is±30 %

Instrument thermal interface	Thermal path	Cold Case heat flux (W)	Hot Case heat flux (W)
IOB to TOB	Conductive heat leaks from IOB to TOB	0.020	–0.030
Cold radiator	Conductive heat leaks from spacecraft	0.005	0.030
	Conductive load from detectors	0.050	0.080
	Net heat flux rejected to Space	0.050	0.100
JT cold-end	Conductive links from L/MWIR modules	0.060	0.130

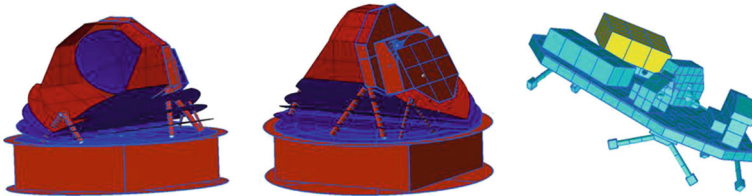


Fig. 14 EChO geometric model views. *Left:* the EChO S/C geometrical model. *Middle:* rear view with the cold radiator on top of the instrument box. *Right:* a view of the instrument optical bench geometric model with the main units

The radiative case is run simulating one position in the solar L2 orbit at a distance of 151.5×10^6 Km. The radiative exchange factors resulting from the geometrical simulations are the input for the thermal case definition. The final simulation is run with the same active loads assumption of the reduced model. In Table 6 are reported the average temperatures at steady state conditions.

The main units temperature is graphically shown also in Figs. 15 and 16. The results in terms of temperature distribution are very encouraging: they show very small gradients between the units and the respective interfaces. This yields some extra margin for further optimization of the interfaces.

Table 6 TMM/GMM Units average temperature

System	Sub-system	Unit	T (K)	System	Sub-system	Unit	T (K)
SVM	Solar array		313.0	Instrument	Optical bench		37.5
	SVM average		249.3		FGS	Box	37.6
VGroove1			148.8			Detectors	35.0
VG2			93.0			FEE	37.7
VG3			48.3	VNIR	Box	37.5	
Telescope	Mirror 1		33.3			Optics	37.5
	M2		33.4		Detectors	35.0	
	M3		33.3		FEE	37.7	
	M4		33.3	SWIR	Box	37.6	
	Optical Bench		33.3			Optics	37.6
	Baffle		32.9		Detectors	35.0	
						FEE	37.7
				MWIR	Box	37.0	
						Optics	28.0
						Detectors	28.2
						FEE	37.6
				LWIR	Box	36.0	
						Optics	28.2
						Detectors	28.2
						FEE	37.6
				Radiator			34.7

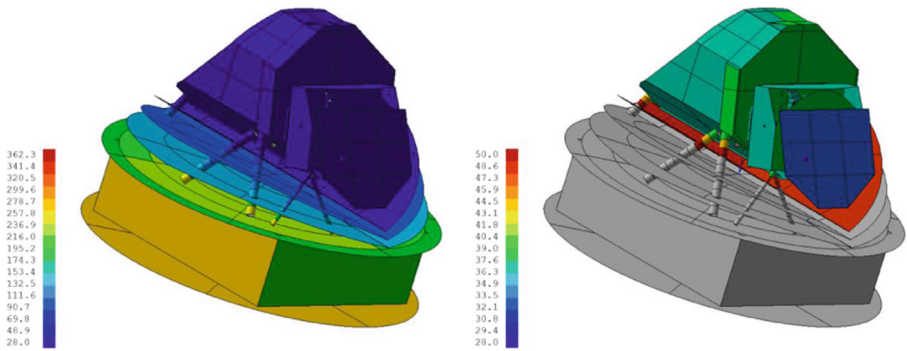


Fig. 15 PLM model: spacecraft average temperatures (*left*); cold PLM main units temperature (*right*)

The net heat loads across the Instrument interfaces are evaluated by balancing the input/output heat fluxes to/from each node through all conductors. For the instrument internal thermal analysis the main interfaces are the Cold Radiator and the JT cooler cold-end. The resulting heat flux values, compared to the simplified model ones, are reported in Table 7.

It is important to notice that even in the worst case of boundary conditions and parasitic leaks the total load on the JT cold end is well below the estimated heat lift capacity of the cooler (200 mW). If this numbers will be confirmed in more advanced design phases, it will be possible to relax the heat load requirement to the cold end heat exchangers and optimize the cryochain performance in a narrower range. The cold radiator rejects more than 60 mW to space while, for the colder channels, almost 40 mW are loaded to the cooler cold heat exchanger.

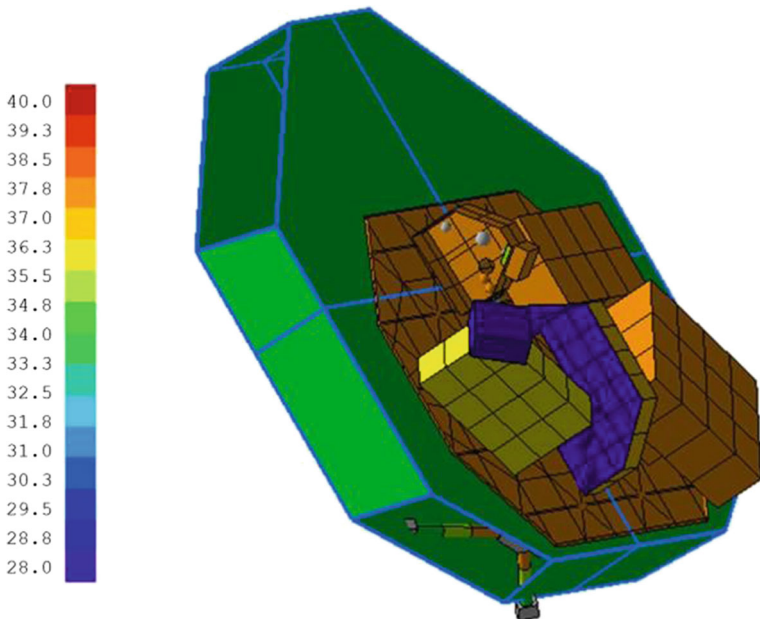


Fig. 16 PLM model: instrument optical bench and module boxes temperature

Table 7 PLM conductive and geometric model: heat fluxes at the instrument main internal thermal interfaces and comparison with the reduced model. An uncertainty of $\pm 30\%$ is assumed on all model results

Instrument thermal interface	Thermal path	PLM T/GMM Heat fluxes (W)	Reduced TMM Cold Case heat fluxes (W)
Cold radiator	Conductive heat leaks from spacecraft	0.006	0.005
	Conductive load from detectors	0.043	0.047
	Radiative load from warmer stages (VG3 and SVM)	0.014	NA
	Net heat flux rejected to Space	0.063	0.052
JT cold-end	Conductive links from L/MWIR modules	0.040	0.055

An important result of the Geometrical Model is to show how the whole spacecraft radiative design is really efficient in rejecting heat, taking full advantage of the L2 favourable thermal conditions. The Telescope Optical Bench, the Telescope Baffle and the Instrument Cold Radiator work together as a single large surface, representing the coldest radiative stages in the spacecraft, at a temperature lower than 40 K, several degrees colder than the last V-Groove. These results indicate, as expected, that the PLM thermal steady state conditions seem to approach the Cold thermal case. The results of the two models look consistent: numbers are in line, taking into account the uncertainties in units and interfaces design. This agreement provides another demonstration of the validity of the thermal design of the EChO instrument integrated in the spacecraft.

5 Thermal stability analysis

Stable conditions during observations are a key requirement for the scientific objectives of EChO. For this reason, thermal stability is one of the key drivers of the mission design. There are two possible thermal noise sources in the EChO PLM: the radiators (V-Grooves and instrument radiator) and the cooler cold end. The main cause of fluctuations on a radiator facing the cold sky is due to orbital changes of the Solar Aspect Angle (SAA) related to flight dynamics following the mission scanning strategy (on timescales of 10 h or so) or seasonal variations (typically on longer periods like weeks, months, years). Experience on previous missions [5], testing [8] and simulations shows that such low frequency oscillations can be controlled under 200 mK over timeframes of 10 h to avoid the thermal background stability becoming a major contributor in the instrument noise budget. The most significant temperature variation will happen when the Sun aspect angle changes while slewing to observe a new science target. Constraints on the maximum slew angle between successive targets ($<36^\circ$ around the Y axis of Fig. 1) are set to limit the SAA changes and the induced temperature variation to less than 10 K in the SVM top floor. This variation is further damped by more than 2 orders of magnitude at the PLM level, well below the temperature stability requirement as demonstrated by analysis and simulations. As a

result, it is not anticipated that significant temperature regulation is needed for the units inside the SVM.

In a JT cooler, instabilities at the reference heat exchanger temperature are due to compressor modulation, with its typical high frequency spectrum (30–40 Hz range), to cold-end internal mass flow 1- or 2-phase dynamics (on the order of tens of seconds) and to precooling stage variations (low frequency).

Thermal stability of the optical modules directly connected to the IOB (FGS, VNIR and SWIR) is not expected to be a major concern given the typical instabilities of passive radiators in L2 either on the timescales of EChO detectors average exposure or on the seasonal. Even in the case of few hundreds of mK peak to peak fluctuations every several hours (10,000 s time scale), the thermal inertia of the instrument bench and modules can damp them well below the required 0.5 K peak to peak.

On the contrary, the detectors are directly connected to their temperature reference and the level of transmitted fluctuations could be at the limit of the required values. Since FPA stability is a key issue for instrumental performance, a careful design of a proper thermal control system is needed. This is achieved by a combination of passive and active systems. The passive component again uses the thermal inertia of the detector system components (struts and frames) to damp temperature oscillations during their propagation from the instability source (the 45 K radiator or the 28 K cold end) to the detectors. As already described in paragraph 2.3, the finer active control is accomplished by a Proportional-Integral-Derivative (PID) type controller on a stage thermally decoupled with a properly tuned resistance between the detectors and the source of temperature oscillations (Fig. 6). Since active control on detectors stage is critical for instrument performance, a fully redundant system with two identical heater and sensor pairs is foreseen.

To verify the functionality of the active control stages design on the EChO modules, analytical studies correlated with a set of transient simulations have been carried out. If periodical thermal instabilities can be approximated with a sinusoidal function and imposed at the relevant interfaces, then the temperature fluctuations transmitted passively at the sensitive stages (the TCS for example) connected to the thermal noise source can be approximated by

$$\Delta T_{\text{TCS}} \cong \frac{\Delta T_0}{\sqrt{1 + \omega^2 R_{\text{TCS}}^2 C_{\text{TCS}}^2}} \cos(\omega t + \varphi)$$

where C_{TCS} is the thermal capacitance of the stage, $R_{\text{TCS}} = 1/G_{\text{TCS}}$ is the resistance between the TCS and the source of the instabilities (cold radiator or the cooler cold end) and ω is the pulsation of the oscillations. The damping factor RC depends on the thermal mass of the stage and on the thermal break with the noise source. Since the thermal inertia of the Temperature Control Stages designed for the EChO detectors is very small, the thermal resistance becomes the key parameter for oscillations passive damping. The conductance value between the detector TCS and its temperature reference is selected on the basis of a trade-off between the detectors operating temperature and the minimum power needed to achieve thermal control at the TCS.

In Tables 8 and 9 are reported some conservative predictions of the possible fluctuations expected at the cold radiator interface and the cooler cold end heat exchangers on

the basis of the trend analysis on cooling stages from previous missions. Planck thermal data [5, 8], for example, indicate that typical instabilities on radiators in L2 can be as high as 10 mK over about 1000 s (because of possible cooler mass flow changes) that can increase to the 100 mK range during change of SAA due to major pointing manoeuvres. As this first analysis has the objective of providing safe and reliable figures for the thermal oscillations at various stages, it has been decided to assume conservative numbers in terms of the frequency components of the expected oscillations spectrum. These are reported in the first three columns of the following tables. The other columns show the level of the transmitted fluctuations evaluated at the Temperature Control Stages (TCS) and on the Detector Systems (DS) of the 45 K and 28 K focal planes.

As expected, this preliminary analysis shows how the thermal design of the units allows for an efficient passive filtering of most of the higher frequency noise. From this follows that all possible oscillations generated in the cooler due to both compressor operations and cold end fluid dynamics (ν in the 10^1 – 10^{-1} Hz range) are filtered out down to negligible levels by the thermal inertia and resistance of the systems. Only the slower oscillations, mainly due to changes related to flight dynamic issues, pass through and need to be actively controlled. The last two columns in each table report the maximum and average proportional control power needed to control the transmitted fluctuations below the required level.

To verify the results of this analysis and to check the robustness of the EChO channels thermal design, a set of simple transient simulations have been run. Sinusoidal oscillations that include the frequency components reported in Tables 8 and 9 have been imposed at the 45 K and 28 K channels detector interfaces. Dynamical simulations, performed using the ESATAN PID routine, show that the active control system can effectively damp the residual oscillations well below the requirements (see Fig. 17). The average power for thermal control on both stages is within the required 5 mW: few mW are dissipated on the 45 K detectors control stage, while the colder detectors need few hundreds of μ W.

In general, thermal stability at the required level of control during routine operation will be achieved by the EChO thermal design, exploiting the L2 favourable radiative environment. Unstable thermal transient states of the S/C, that might be experienced during LEOP, can expose PLM units to undesired conditions. For example, as anticipated, depending on the launch date and time there is the possibility of direct solar illumination of the PLM for durations that can be as long as tens of minutes. To evaluate the impact of such conditions, a preliminary analysis of the possible evolution of the spacecraft thermal balance in the early phases of mission (launch and L2 orbit

Table 8 Spectral components of worst case temperature fluctuation at 45 K detectors stage

Time (s)	ν (Hz)	p-p ΔT (K) at radiator	ΔT at 45 K TCS (K)	ΔT at 45 K DS (K)	Control power max (W)	Control power ave (W)
10	0.1	0.002	3E-05	1E-06	0	0
100	0.01	0.005	0.0008	0.0003	5E-05	3E-05
1000	0.001	0.01	0.0048	0.0046	0.0003	0.0002
10,000	0.0001	0.1	0.0500	0.0500	0.0030	0.0020

Table 9 Spectral components of worst case temperature fluctuation at 28 K detectors stage

Time (s)	ν (Hz)	p-p ΔT at cold end (K)	ΔT at 28 K TCS (K)	ΔT at 28 K DS (K)	ΔT at cold optics	Control power max (W)	Control power ave (W)
10	0.1	0.00002	0.00001	8E-07	2E-08	0	0
100	0.01	0.00005	0.00003	2E-05	4E-07	0	0
1000	0.001	0.0001	0.00005	5E-05	9E-06	0	0
10,000	0.0001	0.001	0.0005	0.0005	0.0004	0.0004	0.0001

injection) has been started. If direct solar exposure is confirmed, the high emissivity surfaces of the PLM units shall be coated by space-qualified white paints to maintain the required IR emissivity (~ 0.9) while reducing solar absorptance (in the 0.1–0.2 range). By adopting such solutions and minimizing the exposure to sunlight, it is possible to ensure thermal performance and avoid critical overheating of the units. Active cooling chain will be off during launch and shall be activated once the pre-cooling stage on the V-Grooves reach the operating temperature. Passive cooling scenarios have been studied

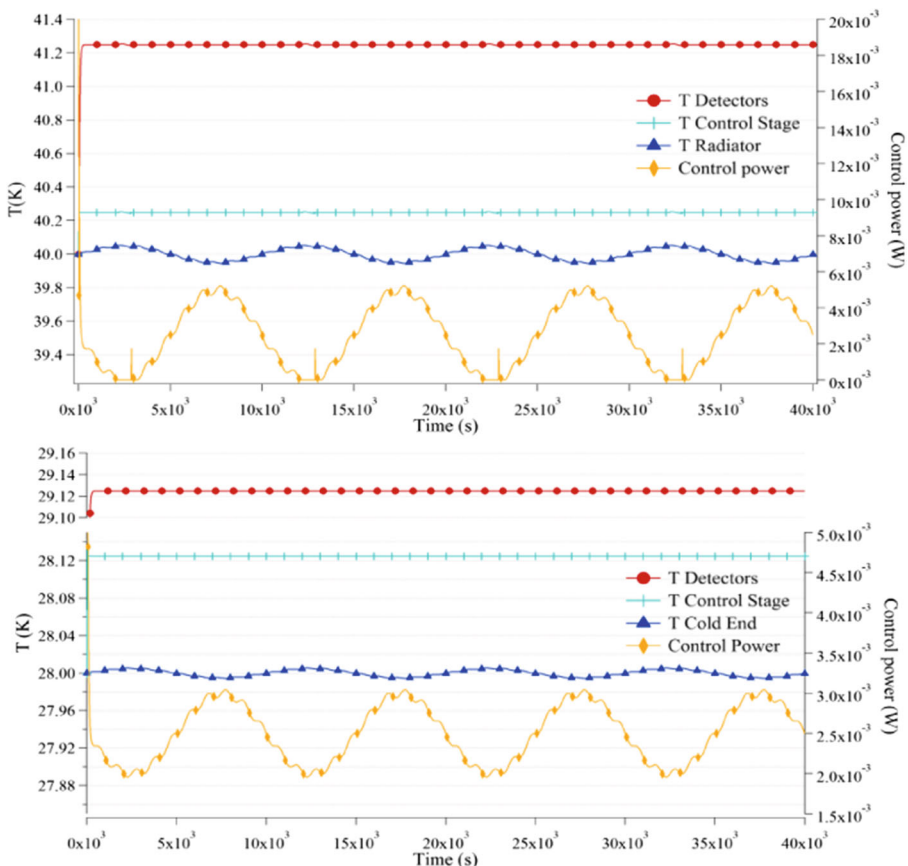


Fig. 17 Simulation of transmitted oscillations to the 45 K (*top*) and 28 K (*bottom*) stage thermal control

correlating the experience and the data of previous missions such as Planck with the EChO thermal design. Assuming an orbit injection similar to previous satellites operating in L2, passive cooling starts right after launch with typical cool-down rate of the radiators on the order of few K per hour. This means that passive stages can reach their equilibrium temperature just few days after insertion into the transfer orbit. Even if this cooling rate should be sufficient to ensure a safe cool-down of the critical units, such as optics and detectors, in terms of mechanical stresses, still it is required to avoid condensation of contaminants (e.g. water) on the sensitive surfaces. For this reason, heaters are mounted on critical elements for cooling regulation and contamination control. After two weeks of outgassing and decontamination, heaters are switched off and the passive cooling is restarted, reaching the equilibrium temperature of the stages in a matter of days. The active cryochain can then be turned on with an expected cool-down time of a week. In total, approximately a month after launch, the main passive stages and the active cold end can be at their operating temperature and ready to start the instrument calibration and verification phase.

6 Conclusions

We presented the baseline thermal architecture of the EChO payload at the end of the study phase for mission down selection. The thermal design is based on the instrument main requirements, flowed down to each unit to identify and configure the main thermal interfaces to the spacecraft and internal to the payload. The required thermo-mechanical properties of units and interfaces have been described. The expected performance of the whole PLM thermal control system has been analysed on the basis of simulations in steady state and transient conditions. The results indicate that the present design is compliant to the instrument and interface requirements for temperature control and heat fluxes.

Typically the margins assumed in this early design phase add up indicating that there is still room for further optimization of the architecture. In the development of the EChO instrument study a more realistic assessment of margins shall be carried out to avoid over design issues. Simulations show that, in the present configuration, the average temperatures of PLM units in steady state conditions are in general well within requirement. Passive cooling performance predictions seem to indicate that the thermal design is very efficient in radiative heat rejection, taking full advantage from the L2 favourable conditions. Heat fluxes are all within the allocation at the passive and active cooling stages, suggesting that a relaxation of requirements on the cryochain shall be possible.

The thermo-mechanical layout of the detectors temperature control stage seems to be efficient and compliant in terms of final stability and power dissipated. Transient simulations, based on instability levels observed in similar missions, indicate that the simple design of the active PID stages is able to filter out and control the expected thermal noise in the time scales typical of EChO scientific observations.

The EChO thermo-mechanical architecture shares the same modular philosophy of the instrument. Parametrical analyses provide the guidelines for scaling and tuning the design to adapt to a relatively wide range of possible evolutions of the instrument.

In general, the thermal architecture here described provides a solid basis for future development of the instrument or mission design.

Acronyms list

<i>ASI</i>	Agenzia Spaziale Italiana (Italian Space Agency)
<i>ASIC</i>	Application Specific Integrated Circuit (electronics)
<i>AWG</i>	American Wire Gauge (wires size)
<i>CAD</i>	Computer Aided Design (drawing software)
<i>CCE</i>	Cooler Control Electronics
<i>CFEE</i>	Cold Front End Electronics
<i>CFRP</i>	Carbon Fibre Reinforced Plastic
<i>DS</i>	Detector System
<i>EChO</i>	Exoplanet Characterization Observatory
<i>EMI</i>	Electromagnetic Interference
<i>ESA</i>	European Space Agency
<i>FEE</i>	Front End Electronics
<i>FGS</i>	Fine Guiding Sensor
<i>FPA</i>	Focal Plane Assembly
<i>FPU</i>	Focal Plane Unit
<i>G</i>	Conductance (thermal)
<i>GFRP</i>	Glass Fibre Reinforced Plastic
<i>GMM</i>	Geometrical Mathematical Model
<i>HXCG</i>	Heat exchanger
<i>ICU</i>	Instrument Control Unit
<i>IOB</i>	Instrument Optical Bench
<i>IR</i>	InfraRed
<i>INAF</i>	Istituto Nazionale di AstroFisica
<i>JT</i>	Joule-Thomson (cooling)
<i>JWST</i>	James Webb Space Telescope
<i>LEOP</i>	Launch and Early Orbit Phase
<i>LWIR</i>	Long Wavelength InfraRed instrument
<i>LVDS</i>	Low Voltage Differential Signaling (harness type)
<i>MCT</i>	Mercury Cadmium Telluride (detectors)
<i>MIRI</i>	Mid InfraRed Instrument (JWST instrument)
<i>MLI</i>	Multi-Layer Insulation
<i>MWIR</i>	Mid Wavelength InfraRed instrument
<i>OM</i>	Optical Module
<i>PID</i>	Proportional-Integral-Derivative (control loop)
<i>PLM</i>	PayLoad Module
<i>PTFE</i>	Polytetrafluoroethylene (Teflon)
<i>R</i>	Resolution (spectral)
<i>RAL</i>	Rutherford Appleton Laboratory (UK)
<i>RC</i>	Resistance Capacitance
<i>S/C</i>	Spacecraft
<i>SAA</i>	Solar Aspect Angle
<i>SS</i>	Stainless Steel
<i>SVM</i>	Service Module
<i>SWIR</i>	Short Wavelength InfraRed instrument
<i>TBC</i>	To Be Confirmed

<i>TCS</i>	Temperature Control Stage
<i>TIF</i>	Thermal InterFace
<i>TMM</i>	Thermal Mathematical Model
<i>TMS</i>	Thermal Modelling Suite
<i>TOB</i>	Telescope Optical Bench
<i>UK</i>	United Kingdom
<i>VG</i>	V-Groove (shielding radiator)
<i>VNIR</i>	Visible and Near InfraRed instrument
<i>WE</i>	Warm Electronics

Acknowledgments We want to acknowledge here the fundamental contribution of the EChO system team to this work. The Italian participation to the EChO mission was supported by the Italian Space Agency (ASI) in the framework of the ASI-INAF agreement “Missione EChO: assessment phase”, I/022/12/0.

References

1. Tinetti, G., et al.: EChO. Exoplanet characterisation observatory. *Exp. Astron.* **34**(2), 311–353 (2012)
2. EChO Yellow Book, ESA SRE 2013 2 EChO, (2013)
3. Eccleston, P., et al.: EChO Assessment Study Design Report, ECHO-RP-0001-RAL, Issue 3.0 (2013)
4. Focardi, M., Farina, M., Pancrazzi, M., Di Giorgio, A. M., Pezzuto, S., Ottensamer, R., Pace, E., Micela, G.: EChO electronics architecture and SW design. *Experimental Astronomy EChO Special Issue*, submitted (2014)
5. Planck collaboration: Planck early results. II. The thermal performance of Planck. *Astron. Astrophys.* **536**, A2 (2011)
6. Shaughnessy, B. M., Eccleston, P.: Thermal Design of the Mid-Infrared Instrument (MIRI) for the James Webb Space Telescope. International Conference on Environmental Systems (ICES) 2008, San Francisco, California, USA, paper 2009-01-2410 (2009)
7. Morgante, G., Terenzi L.: EChO TMM/GMM Description and Results Technical Note, ECHO-TN-0001-IASFBO, Issue 1.0 (2013)
8. Morgante, G., et al.: Cryogenic characterization of the Planck sorption cooler system flight model. *J. Inst.* **4**, T12016 (2009)